Hall, P. W. Keaton, Jr., and M. P. Kellogg, Nucl. Instr. Methods 70, 69 (1969).

[16]P. McWilliams, W. S. Hall, and H. E. Wegner, Rev. Sci. Instr. 33, 70 (1962).

[17]S. Kobayaski, J. Phys. Soc. Japan 15, 1164 (1960).

[18]G. Hardie, Ph.D. dissertation, University of Wisconsin, 1962 (unpublished).

[19]W. W. Daehnick, Phys. Rev. 135, B1168 (1964).

[20]Y. Nagahara, J. Phys. Soc. Japan 16, 133 (1961).

[21]W. W. Daehnick and R. Sherr, Phys. Rev. 133, B934 (1964).

[22]J. K. Dickens, D. A. Haner, and C. N. Waddell, Phys. Rev. 132, 2159 (1963).

[23]L. Rosen, J. G. Beery, A. S. Goldhaber, and E. H. Auerbach, private communication.

[24]A. G. Worthing and J. Geffner, *Treatment of Experi-*

mental Data (John Wiley & Sons, Inc., New York, 1943), pp. 201–202.

[25]J. F. Dicello, Los Alamos Scientific Laboratory Report No. LA-3842, 1968 (unpublished).

[26]A. G. Blair and D. D. Armstrong, private communication.

[27]B. W. Ridley and J. F. Turner, Nucl. Phys. 58, 497 (1964).

[28]L. N. Blumberg, E. E. Gross, A. van der Woude, A. Zucker, and R. H. Bassell, Phys. Rev. 147, 812 (1966).

[29]J. F. Turner, B. W. Ridley, P. E. Cavanagh, G. A. Gard, and A. G. Hardacre, Nucl. Phys. 58, 509 (1964).

[30]J. G. Kelly, D. E. Heagerty, H. G. Graetzer, and D. A. Lind, unpublished.

Nuclear Structure of ^{22}Na: The ^{23}Na(^{3}He, α) Reaction*

J. D. Garrett,† H. T. Fortune, and R. Middleton

Physics Department, University of Pennsylvania, Philadelphia, Pennsylvania 19104

(Received 10 May 1971)

The states of ^{22}Na below 7.5 MeV have been studied using the ^{23}Na(^{3}He, α)^{22}Na reaction at a bombarding energy of 18 MeV. Angular distributions of the reaction products have been compared with distorted-wave Born-approximation predictions. The resulting spectroscopic factors are compared with those calculated using the rotational model and with experimental spectroscopic factors from the ^{23}Na(p,d) and ^{23}Na(d,t) reactions. The results suggest a $K^\pi = 1^-$, $T = 0$ rotational band (2.21 MeV, 1^-; 2.57 MeV, 2^-; and 3.52 MeV, 3^-) and a $K^\pi = 2^-$, $T = 0$ band [4.58 MeV, 2^- ($0^-, 1^-, 3^-$) and 5.44 MeV, $3^-(0^-, 1^-, 2^-)$] based on neutron pickup from the $\frac{1}{2}^-$[101] Nilsson orbit. A comparison of the $l = 1$ ^{23}Na(^{3}He, α) transition to the 5.95-MeV level in ^{22}Na with the ^{23}Na($d, ^3$He)^{22}Ne results suggests that this state is the analog of the 5.14-MeV, 2^- state in ^{22}Ne and that these levels correspond to the $K^\pi = 2^-$, $T = 1$ band head based on nucleon pickup from the $\frac{1}{2}^-$[101] Nilsson orbit. The results of the present study and a previous ^{21}Ne(^{3}He, d)^{22}Na study are discussed in terms of Nilsson configurations and associated rotational bands. It is found that the rotational model provides a reasonably adequate explanation for the observed spectroscopic factors of the negative-parity states up to 7.5 MeV and for the positive-parity states based on the $(\frac{3}{2}^+[211])^2$ configuration if a deformation of $\delta \approx 0.5$ is assumed. The simple rotational model, however, is unable to account for the observed single-nucleon-transfer spectroscopic factors for the other positive-parity configurations.

I. INTRODUCTION

The nuclear structure of ^{22}Na is of current experimental interest.[1-5] The nuclei in this mass region are believed to be among the most deformed.[1,2,6-9] The low-lying states of ^{22}Na have been described as rotational bands based on Nilsson configurations.[1,2,5,6] The suggested rotational bands and the known spins and parities of the states of ^{22}Na are summarized in Ref. 1. The results of γ-ray decay studies for the levels of ^{22}Na below 5.2 MeV are summarized in Ref. 5. Limits on the lifetimes of the levels below 3.1 MeV have also been determined.[10-17] Spectroscopic information for the bound states of ^{22}Na is available from

the ^{21}Ne(^{3}He, d)[1] and ^{20}Ne(^{3}He, p)[2] stripping reactions. Single-nucleon-pickup reactions [^{23}Na-(p, d)[18] and ^{23}Na(d, t)[19,20]] have been performed leading to states below 2.6-MeV excitation in ^{22}Na.

In the present study the states of ^{22}Na up to 7.5-MeV excitation were studied using the ^{23}Na(^{3}He, α) reaction at an incident energy of 18 MeV. The angular distributions of α-particle groups have been compared with distorted-wave Born-approximation (DWBA) predictions. The resulting experimental spectroscopic factors were then compared with spectroscopic factors calculated using Nilsson-model wave functions. The levels of ^{22}Na are discussed in terms of Nilsson configurations and their associated rotational bands.

II. EXPERIMENTAL PROCEDURE AND RESULTS

The ^{23}Na(^{3}He, α)^{22}Na reaction was studied at an incident energy of 18 MeV using the ^{3}He beam from the University of Pennsylvania tandem Van de Graaff accelerator. Reaction products were momentum-analyzed in $3\frac{3}{4}°$ intervals between $3\frac{3}{4}$ and 75° (lab) by performing two exposures in a multi-angle spectrograph. The α particles were detected photographically in 50-μm Ilford K-1 nuclear emulsions. The target was 35 μg/cm^2 of NaI on a 20-μg/cm^2 natural C backing.

An α-particle momentum spectrum obtained at a laboratory angle of $3\frac{3}{4}°$ is shown in Fig. 1. Reaction products resulting from the carbon backing and ^{16}O impurities are identified by the levels of the corresponding residual nucleus. Angular distributions of 53 α-particle groups leading to states of ^{22}Na below 7.5 MeV are shown in Figs. 2–6. The error bars shown on the data points represent the larger of the statistical errors and 5%. An additional error of 30%, due principally to uncertainty in target thickness, is assigned to the absolute cross-section scale.

III. ANALYSIS

The analysis of the angular distribution was performed using the DWBA code DWUCK.[21] For a single-particle-pickup reaction, the experimental cross section, $\sigma_{\exp}(\theta)$, is related to the theoretical single-particle cross section (calculated using code DWUCK), $\sigma_{nlj}(\theta)$, by the expression

$$\sigma_{\exp}(\theta) = NC^2 \sum_{nlj} S_{nlj} \frac{\sigma_{nlj}(\theta)}{2j+1}, \qquad (1)$$

where

$$C = \langle T_f T_{zf} t t_z | T_i T_{zi} \rangle. \qquad (2)$$

Here T and T_z are the isospin and z component of isospin, respectively, i and f refer to the target and residual nucleus, and n, l, j, t, and t_z are quantum numbers of the transferred particle. The normalization factor, N, which includes the overlap of the incident and exciting particle wave functions, is not well determined for the (^{3}He, α) reaction.[22] The value of N will be discussed further in Sec. IV. For a (^{3}He, α) reaction on a $T = \frac{1}{2}$ target, the isospin Clebsch-Gordon coefficient has the value $C^2 = 1$
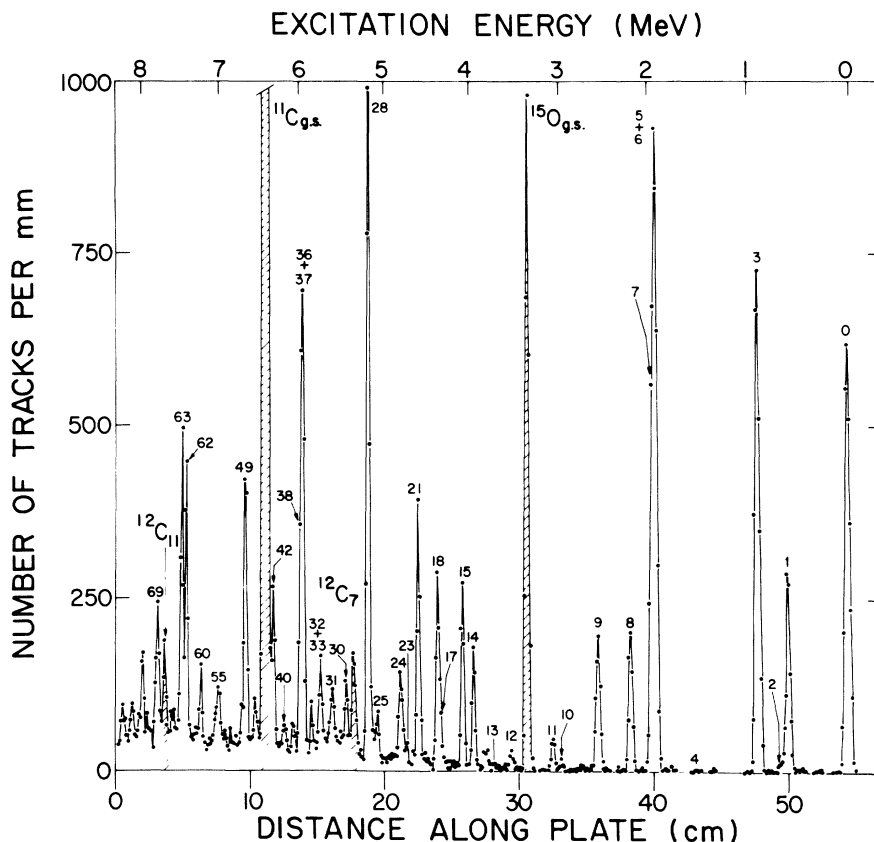

FIG. 1. α-particle energy spectrum for the reaction ^{23}Na(^{3}He, α)^{22}Na at a bombarding energy of 18.0 MeV and a laboratory angle of $3\frac{3}{4}°$.

for transitions to $T = 0$ final states and $C^2 = \frac{1}{3}$ for transitions to $T = 1$ final states. The spectroscopic factor, S_{nlj}, is a measure of the overlap of the target with the final state of the residual nucleus plus transferred particle.

The appropriate elastic scattering measurements were not available to determine the entrance- and exit-channel optical-model parameters. However, for light deformed nuclei, better results are usually obtained in DWBA calculations by the use of average optical-model parameters applicable to the given energy and mass region.

The optical-model parameters used in the present analysis (given in Table I) have been successfully used in the region of the Ne, Mg, and Si isotopes.[22, 23] The principal feature of the large value of V_{so} is that it was necessary to reproduce the observed J dependence in $l = 2$ transitions in (^{3}He, α) reactions on the Mg and Si isotopes.[23] Its effect on spectroscopic factors is negligible.

The DWBA calculations were performed in the zero-range approximation using local potentials and a lower-cutoff radius of zero on the radial integrals. All the calculations were performed

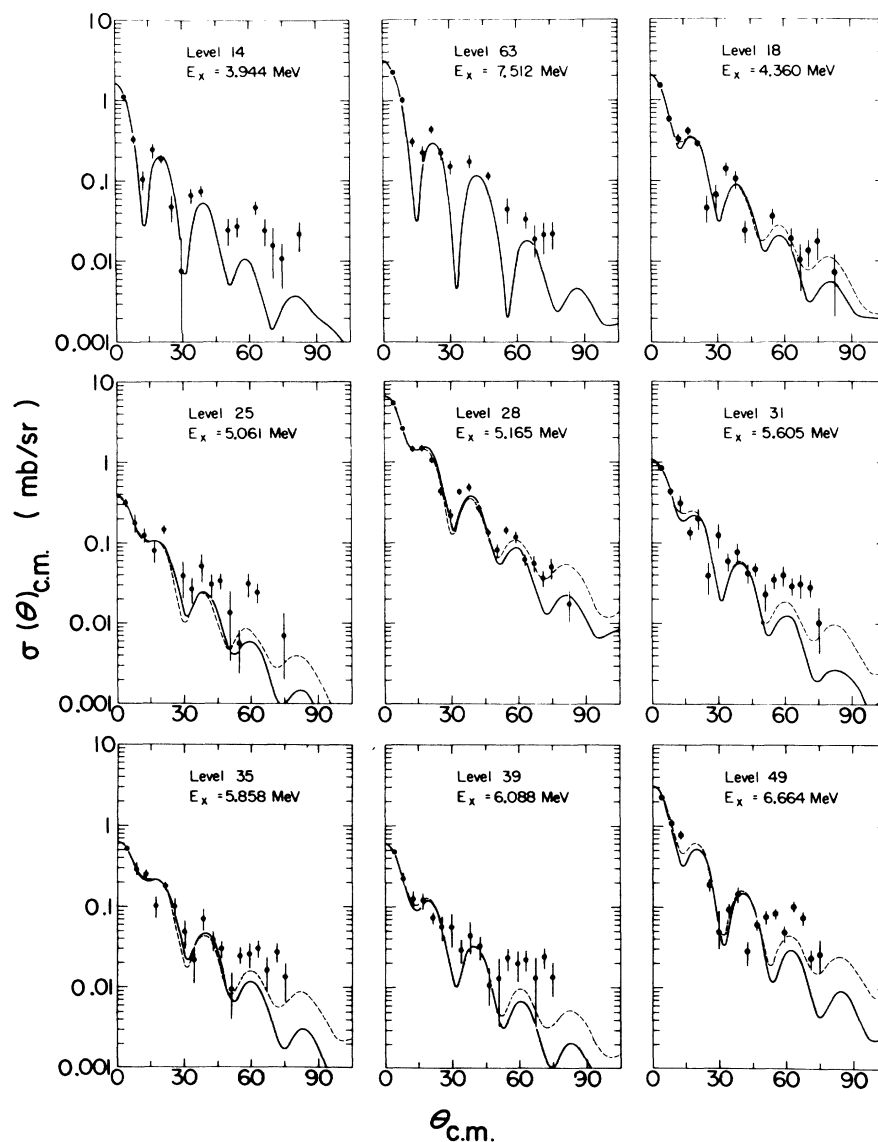

FIG. 2. Angular distributions exhibiting pure $l = 0$ and $l = 0 + 2$ admixed character in the ^{23}Na(^{3}He, α) reaction. The DWBA curves shown for levels 14 and 63 were calculated for pure $l = 0$ transitions. The remaining levels are shown with admixed $l = 0$ and 2 predictions. The solid and dashed curves correspond, respectively, to $1d_{5/2}$ and $1d_{3/2}$ $l = 2$ components.

using a Thomas spin-orbit strength of $\lambda = 25$ in the bound state even though it is known[22] that this value may lead to a reduced theoretical cross section for $j = l - \frac{1}{2}$.

Extracted spectroscopic factors were compared with those calculated using Satchler's formula[24] for deformed nuclei:

$$C^2 S_{lj} = g^2 \frac{2I_f + 1}{2I_i + 1} |\langle i|f\rangle|^2 |\langle j(K_i \mp K_f)I_f \pm K_f|I_i K_i\rangle|^2$$

$$\times |\langle \chi_i|a^+|\chi_f\rangle|^2, \tag{3}$$

where the parameters are as defined in Ref. 1. The ground state of ^{23}Na, $|\chi_i\rangle$, was assumed to be a proton and two neutrons in the $\frac{3}{2}^+[211]$ Nilsson orbit outside a ^{20}Ne closed core. Values of the matrix element of Eq. (3) are given in Table II. Use of the orthonormality of the Clebsch-Gordon coefficients leads to the in-band sum rules given in column 5 of Table II. The sum is over n, l, and j for all final states in a rotational band.

The Nilsson expansion coefficients, $W(\alpha, \nu)$ ($\alpha = N, n_z, \Lambda$, the Nilsson asymptotic quantum numbers; and $\nu = nljmt_z$, the shell-model quantum

FIG. 3. Angular distributions exhibiting pure $l = 2$ character in the ^{23}Na(^{3}He, α) reaction. The solid DWBA curves correspond to pickup from the $1d_{5/2}$ subshell and the dashed curves from $1d_{3/2}$ subshell. A prediction based on an $l = 1$ transition (dotted curve) is shown for comparison with level 40.
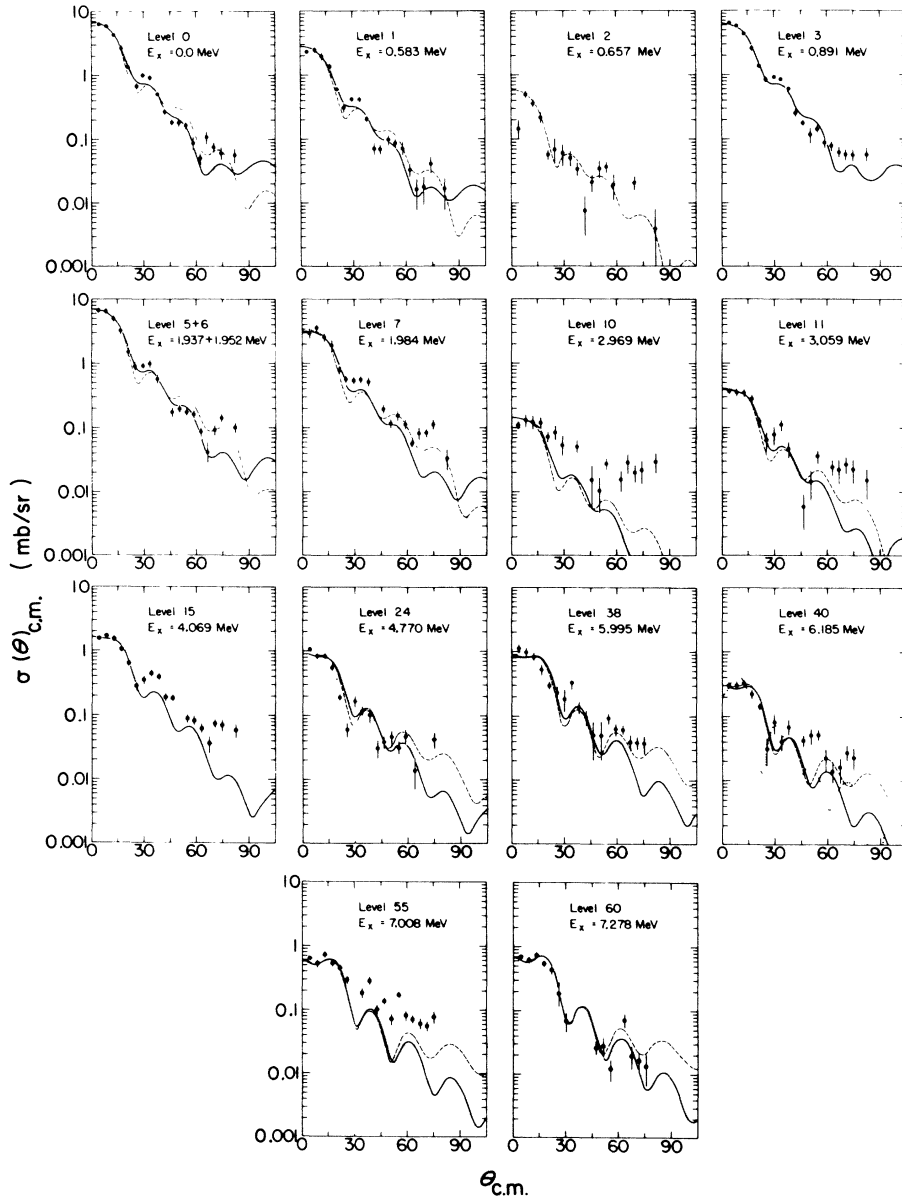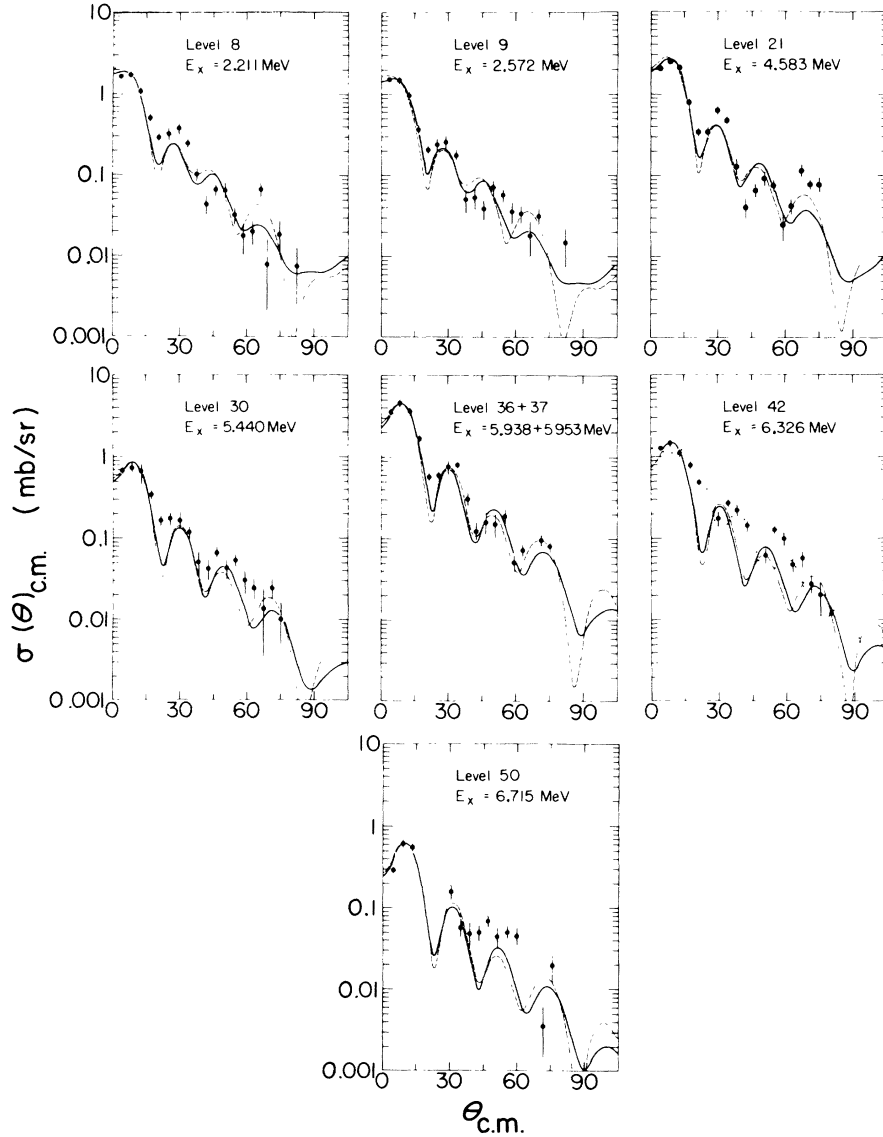
FIG. 4. Angular distributions exhibiting $l = 1$ character in the ^{23}Na(^{3}He, α) reaction. The solid DWBA curves correspond to pickup from the $1p_{3/2}$ subshell, and the dashed curves from the $1p_{1/2}$ subshell. A prediction based on an $l = 2$ transition (dotted curve) is shown for comparison with level 42.

TABLE I. Optical-model parameters used in the DWBA calculations (see Refs. 22 and 23):

$$U(r) = V_C(r, r_C) - V_0 \frac{1}{1+e^x} - iW \frac{1}{1+e^{x'}} + \left(\frac{\hbar}{M_\pi c}\right)^2 V_{so} \frac{1}{r} \frac{d}{dr} \left(\frac{1}{1+e^{x''}}\right) \vec{l} \cdot \vec{\sigma} ;$$

$$x = \frac{r - r_0 A^{1/3}}{a} , \quad x' = \frac{r - r_0' A^{1/3}}{a'} , \quad x'' = \frac{r - r_{so} A^{1/3}}{a_{so}} .$$

Channel	V_0 (MeV)	W (MeV)	$r_0 = r_{so}$ (F)	$a = a_{so}$ (F)	r_C (F)	r_0' (F)	a' (F)	V_{so} (MeV)
^{23}Na + ^{3}He	130.0	24.0	1.31	0.61	1.40	1.43	1.01	10.0
^{22}Na + α	180.0	16.5	1.42	0.56	1.40	1.42	0.56	...
Bound state	a	...	1.26	0.60	...	...	...	$\lambda = 25$

a The bound-state well depths were adjusted to give the nucleons a binding energy of $B = [20.578 - Q(^3$He, $\alpha)]$ MeV.
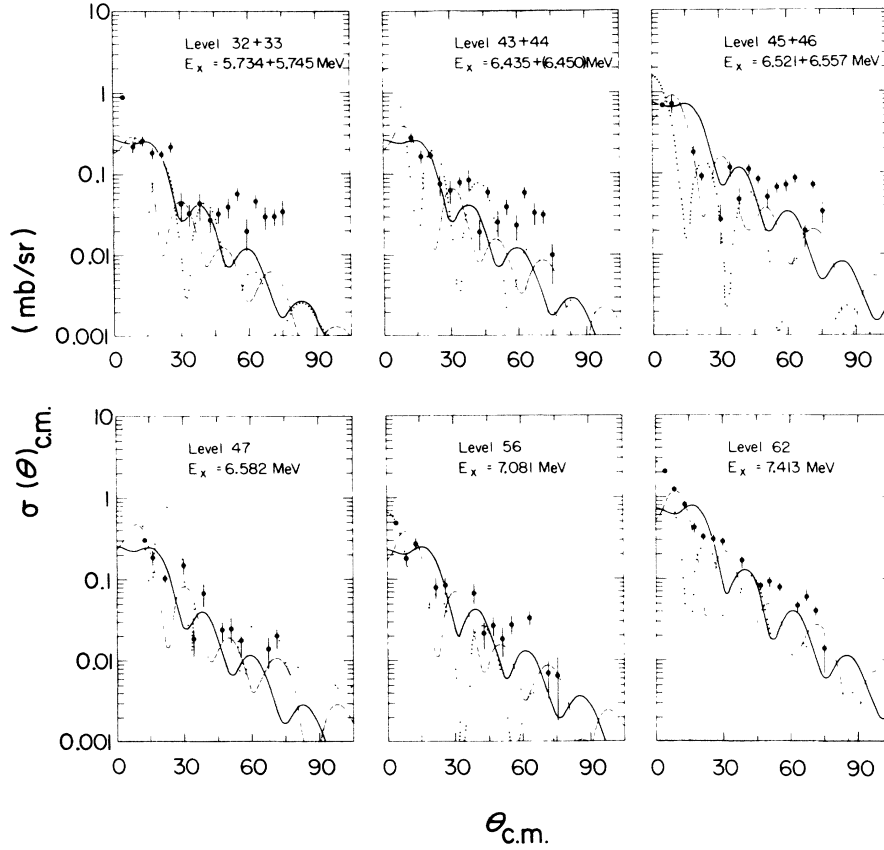
FIG. 5. Angular distributions which exhibit structure characteristic of direct transfer that is not characteristic of an $l = 0$, 1, 2, or $0 + 2$ transition. The dotted, dashed, and solid DWBA curves correspond to $l = 0$, 1, and 2 transitions, respectively.

TABLE II. Matrix elements and sum rules for predicting spectroscopic factors for various configurations [see Eq. (3) and text].

Configuration	K, T	$|\langle \chi_i|a^\dagger|\chi_f\rangle|^2$	g^2	$\sum_{\substack{nlj \\ I_f}} S_{nlj}$ [a]
$(\frac{3}{2}^+ [211])^2$	0, 1	$\frac{1}{2} W(\alpha, \nu)^2$	2	$\frac{3}{2} \sum_{nlj} W(\alpha, \nu)^2$
$(\frac{3}{2}^+ [211])^2$	0, 0	$\frac{1}{2} W(\alpha, \nu)^2$	2	$\frac{1}{2} \sum_{nlj} W(\alpha, \nu)^2$
$(\frac{3}{2}^+ [211])^2$	3, 0	$W(\alpha, \nu)^2$	1	$\sum_{nlj} W(\alpha, \nu)^2$
b	$T = 0$ [c]	$\frac{1}{2} W(\alpha, \nu)^2$	$1 + \delta (K_f, 0)$	$\frac{1}{2} \sum_{nlj} W(\alpha, \nu)^2$
b	$T = 1$ [c]	$\frac{1}{2} W(\alpha, \nu)^2$	$1 + \delta (K_f, 0)$	$\frac{3}{2} \sum_{nlj} W(\alpha, \nu)^2$

[a] For deformed harmonic-oscillator wave function $\sum_{nlj} W(\alpha, \nu)^2 = 1$. For normalization of wave functions calculated using Woods-Saxon potential see text and Refs. 1 and 2.

[b] Configurations where extracore nucleons are not in same Nilsson orbit.

[c] $K = \Omega_1 + \Omega_2$ or $|\Omega_1 - \Omega_2|$.

TABLE III. Results of the ^{23}Na(^{3}He, α)^{22}Na reaction.

Level No.	Literature E_x (MeV $\pm$keV)[a]	J^π[b]	E_x (MeV)[c]	l_n	^{23}Na(^{3}He, α)^{22}Na results Assignment	j_n	NC^2S
0	0.0	3^+	0.0	2		$\frac{5}{2}$	27.0
						$\frac{3}{2}$	40.0
1	0.583 ± 2	1^+	0.577	2		$\frac{5}{2}$	11.1
						$\frac{3}{2}$	16.2
2	0.657 ± 2	0^+, $T=1$	0.651	2		$\frac{3}{2}$	3.24
3	0.891 ± 2	4^+	0.881	2		$\frac{5}{2}$	25.5
4	1.528 ± 2	5^+	1.523	d			
5	1.937 ± 2	1^+	1.942	2		$\frac{5}{2}$	25.8
6	1.952 ± 2	2^+, $T=1$				$\frac{3}{2}$	40.8
7	1.984 ± 2	3^+	1.995[e]	2		$\frac{5}{2}$	12.9
						$\frac{3}{2}$	19.6
8	2.211 ± 2	1^-	2.212	1		$\frac{3}{2}$	9.52
						$\frac{1}{2}$	12.0
9	2.572 ± 2	2^-	2.572	1		$\frac{3}{2}$	7.80
						$\frac{1}{2}$	9.60
10	2.969 ± 2	3^+	2.978[e]	(2)		$\frac{5}{2}$	<0.90
						$\frac{3}{2}$	<1.40
11	3.059 ± 2	2^+	3.059	2		$\frac{5}{2}$	1.68
						$\frac{3}{2}$	2.56
12	3.521 ± 2	3^-	3.526	f		$\frac{3}{2}$	<0.16
13	3.708 ± 2	(6^+)	3.708	d			
14	3.944 ± 2	1^+	3.951	0		$\frac{1}{2}$	1.4
15	4.069 ± 2	$(4)^+$, $(T=1)$	4.067	2		$\frac{5}{2}$	7.8
16	4.294 ± 2			g			
17	4.319 ± 2	1^+	4.317	d			
18	4.360 ± 2	2^+ (1^+)	4.362	0+2		$\frac{5}{2}$	1.16
						$\frac{1}{2}$	1.17
						$\frac{3}{2}$	2.16
						$\frac{1}{2}$	1.12
19	4.466 ± 5		4.465	d			
20	4.522 ± 5		4.534[e]	d			
21	4.583 ± 2		4.583	1	$2^- (0^-, 1^-, 3^-)$[h]	$\frac{3}{2}$	12.0
						$\frac{1}{2}$	15.3
22	4.622 ± 2	1	4.640[e]	d			
23	4.708 ± 3	$(3^+, 4^+, 5^+)$		d			
24	4.770 ± 2	$0^+, 1^+, 2^+, 3^+, 4^+$	4.769	(2)		$\frac{5}{2}$	4.56
						$\frac{3}{2}$	7.20
25	5.061 ± 2	≥ 1	5.063	0+2	$1^+, 2^+$	$\frac{5}{2}$	0.864
						$\frac{1}{2}$	0.256

TABLE III *(Continued)*

Level No.	E_x (MeV ±keV) [a]	J^{π} [b]	E_x (MeV) [c]	l_n	^{23}Na(^{3}He, α)^{22}Na results Assignment	j_n	NC^2S
						$\frac{3}{2}$	1.25
						$\frac{1}{2}$	0.254
26	5.099 ± 5		} 5.115	d			
27	5.117 ± 5						
28	5.165 ± 4	$(2)^+$, $(T=1)$	5.167	0 + 2		$\frac{5}{2}$	6.96
						$\frac{1}{2}$	3.20
						$\frac{3}{2}$	10.6
						$\frac{1}{2}$	3.24
29	5.317 ± 7	1^+, $2^+(0^+$, 3^+, $4^+)$	5.322	d			
30	5.440 ± 7	0^-, 1^-, 2^-, 3^-	5.436	1	$3^-(0^-$, 1^-, $2^-)$ [h]	$\frac{3}{2}$	3.72
						$\frac{1}{2}$	4.90
31	5.605 ± 7	1^+, 2^+	5.600	0 + 2		$\frac{5}{2}$	1.01
						$\frac{1}{2}$	0.528
						$\frac{3}{2}$	1.84
						$\frac{1}{2}$	0.510
32	5.734 ± 15*	One level	} 5.738	i			
33	5.745 ± 15*	0^+, 1^+					
34	5.830 ± 7		5.828 [e]	d			
35	5.858 ± 10		5.865	0 + 2	1^+, 2^+	$\frac{5}{2}$	1.19
						$\frac{1}{2}$	0.254
						$\frac{3}{2}$	1.98
						$\frac{1}{2}$	0.246
36	5.938 ± 15*			j			
37	5.953 ± 15*		5.958	1	{2^-, $(0^-$, 1^-, $3^-)$ [h] $(T=1)$	$\frac{3}{2}$	19.6
						$\frac{1}{2}$	26.4
38	5.995 ± 10	1^+, 2^+	6.004 [e]	2		$\frac{5}{2}$	5.64
						$\frac{3}{2}$	8.96
39	6.088 ± 7	1^+, $2^+(0^+$, 3^+, $4^+)$	6.074 [e]	0 + 2	1^+, 2^+	$\frac{5}{2}$	0.510
						$\frac{1}{2}$	0.288
						$\frac{3}{2}$	0.844
						$\frac{1}{2}$	0.282
40	6.185 ± 7	0^+, 1^+, 2^+, 3^+, 4^+	6.183	(2)		$\frac{5}{2}$	1.95
						$\frac{3}{2}$	3.28
41	6.247 ± 7		6.236	d			
42	6.326 ± 7	1^-, 2^-, $(0^-$, $3^-)$	6.324	(1)		$\frac{3}{2}$	6.48
						$\frac{1}{2}$	8.60
43	6.435 ± 10*		} 6.429	i			
44	6.450 ± 15*						

TABLE III *(Continued)*

Level No.	Literature E_x (MeV ±keV)[a]	J^{π} [b]	E_x (MeV)[c]	l_n	^{23}Na(^{3}He, α)^{22}Na results Assignment	j_n	NC^2S
45	6.521 ± 7	} 1+, 2+ }	6.543	i			
46	6.557 ± 7						
47	6.582 ± 7		6.594 [e]	i			
48	6.640 ± 10 *		6.641 [e]	d			
49	6.664 ± 7	(1+, 2+, 3+)	6.674	(0 + 2)	1+, 2+, (3+)	$\frac{5}{2}$	1.88
						$\frac{1}{2}$	1.46
						$\frac{3}{2}$	4.28
						$\frac{1}{2}$	1.37
50	6.715 ± 7		6.711	(1)	3⁻(0⁻, 1⁻, 2⁻) [h]	$\frac{3}{2}$	2.68
					(T = 1)	$\frac{1}{2}$	3.64
51	6.750 ± 7		6.770 [e]	d			
52	6.834 ± 7	0+ (1+)(T = 1)		g			
53	6.862 ± 7		6.866 [e]	d			
54	6.961 ± 7		6.949 [e]	d			
55	7.008 ± 7		7.000	2	0+, 1+, 2+, 3+, 4+	$\frac{5}{2}$	4.56
						$\frac{3}{2}$	7.00
56	7.081 ± 7		7.075 [e]	i			
57	7.153 ± 7		7.158 [e]	d			
58	7.220 ± 7		7.225 [e]	d			
59	7.242 ± 7			g			
60	7.278 ± 7		7.285	2	0+, 1+, 2+, 3+, 4+	$\frac{5}{2}$	6.94
						$\frac{3}{2}$	8.60
61	7.367 ± 7		7.356 [e]	j			
62	7.413 ± 7		7.403	i			
63	7.512 ± 7			0	1+, 2+	$\frac{1}{2}$	0.169

[a] Energies from Ref. 5 below 5.3 MeV and from Ref. 2 for those above 5.3 MeV except for those marked by an asterisk where they are from Ref. 27.

[b] From the literature as summarized in Refs. 1 and 2.

[c] Expected error, ±10 keV.

[d] No pickup pattern observed (see Fig. 6).

[e] Expected error, ±20 keV.

[f] No pickup pattern observed (see Fig. 6); however, upper limit given for spectroscopic factor based on known J^{π}.

[g] State not excited.

[h] See text for discussion of J^{π} assignment.

[i] See Fig. 5 and Table V.

[j] Covered by neighboring strongly excited state.

numbers of the transferred nucleon), used in the calculation of spectroscopic factors were calculated[1,25] for a proton in a deformed Woods-Saxon well of mass 22. They are tabulated in Ref. 1. The binding energies of the deformed Woods-Saxon potential[1,25] are compared with the harmonic-oscillator results[26] in Fig. 7.

IV. RESULTS

The ^{23}Na(^{3}He, α)^{22}Na angular distributions have been classified into six categories: (1) predominant $l = 0$ (transitions to the 3.944- and 7.512-MeV levels); (2) $l = 0$ and $l = 2$ admixed (Fig. 2 except

for the 3.944- and 7.512-MeV transitions); (3) predominant $l = 2$ (Fig. 3); (4) predominant $l = 1$ (Fig. 4); (5) distributions which show considerable structure but do not fit into categories 1–4 (Fig. 5); and (6) weak cross sections showing little structure (Fig. 6).

In Fig. 2 the 3.944- and 7.512-MeV levels are shown with $l = 0$ DWBA predictions. The remaining transitions in Fig. 2 are shown with admixed $l = 0$ and $l = 2$ calculations. The solid and dashed lines are based, respectively, on $l = 2$ pickup from the $1d_{5/2}$ and $1d_{3/2}$ subshells. The admixtures were determined by means of a χ^2-minimization fit to the
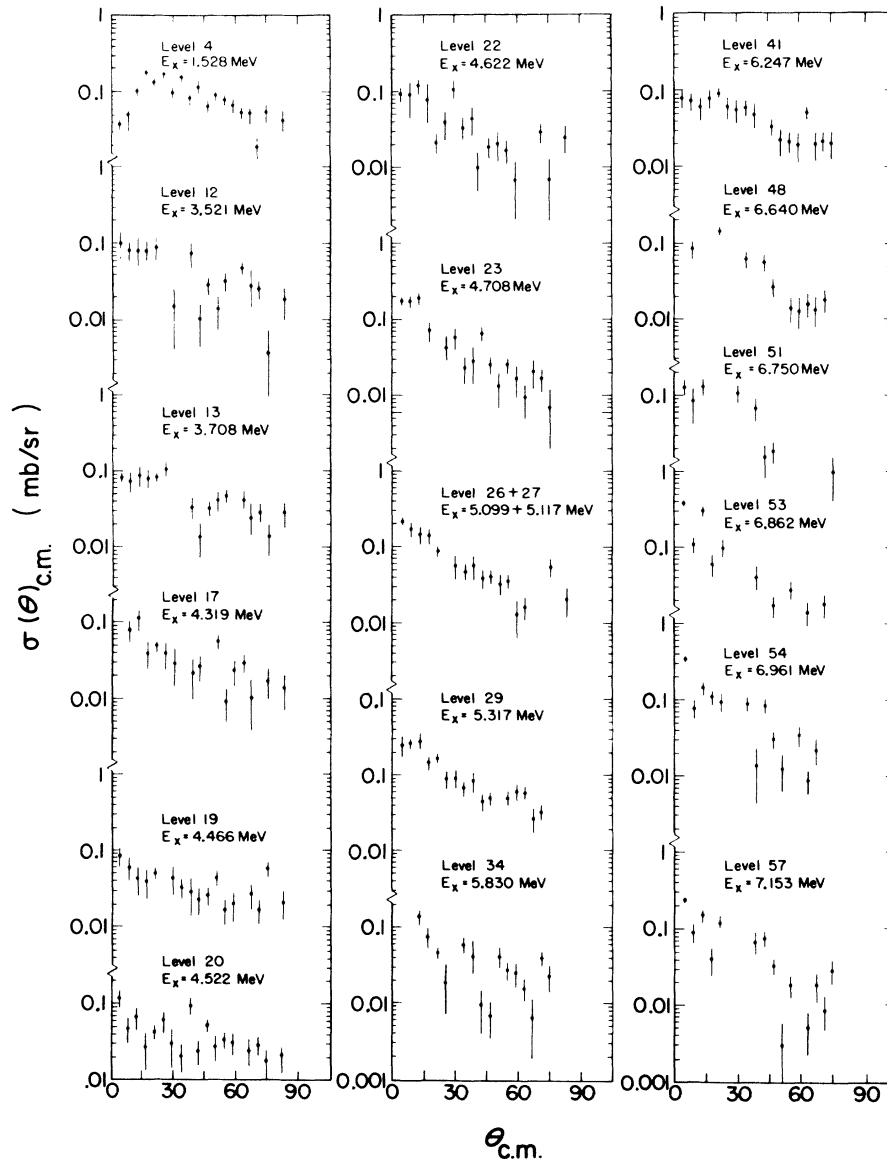

FIG. 6. Angular distributions for states excited weakly in the ^{23}Na(^{3}He, α) reaction that are not characteristic of direct nucleon-transfer reactions.

experimental data. The $l=0$ peak DWBA cross section is an order of magnitude greater than the $l=2$ peak cross section; therefore, a relatively small error in this procedure could produce a large error in the $l=2$ spectroscopic factor. The $l=0+2$ classification of the transition to the 6.664-MeV level should be considered as tentative, since this group was obstructed by reaction products from an impurity at several critical angles near the second maximum.

Transitions characteristic of the transfer of two units of orbital angular momentum are displayed in Fig. 3. The solid and dashed lines correspond to pickup from the $1d_{5/2}$ and $1d_{3/2}$ configurations, respectively. Only one curve is shown with the 0.657-, 0.891-, and 4.069-MeV angular distributions, since known spin-parity assignments for these states limit the transitions to $j_n = \frac{3}{2}$ for the 0.652-MeV level and $j_n = \frac{5}{2}$ for the levels at 0.891 and 4.069 MeV. The angular distribution of the 2.969-MeV state is included with the $l=2$ transitions because of its known spin[6] and parity[5] of $J^\pi = 3^+$, and its $l=2$ ^{21}Ne(^{3}He, d)^{22}Na angular distribution.[1] The agreement between theory and experiment for the 5.995- and 6.185-MeV states is not as good as for the other transitions. Larger error bars on the 5.995-MeV angular distribution are due to large errors in separating this group from the strong transition to the 5.938 + 5.953-MeV doublet. A DWBA prediction based on $l=1$ neutron pickup is shown (dotted line) on the 6.185-MeV angular distribution for comparison. At forward angles the agreement with the $l=2$ predic-

tions is good; however, at larger angles discrepancies exist. This level (6.185 MeV) has previously been suggested[1,27] as a possible doublet.

The angular distributions characteristic of $l=1$ neutron transfer are shown in Fig. 4, the solid and dashed lines corresponding, respectively, to pickup from $1p_{3/2}$ and $1p_{1/2}$ configurations. Only the transitions to the 6.326- and 6.715-MeV states could be in question. An $l=2$ DWBA prediction (dotted line) is shown for comparison with the 6.326-MeV transition. Several experimental points are missing from the angular distribution to the 6.715-MeV state due to reaction products from impurity groups.

The six angular distributions in Fig. 5 exhibit considerable structure but are not characteristic of a pure l transfer or an $l=0+2$ admixture. Three of these distributions are sums of transitions to known unresolved doublets (those at 5.734 + 5.745 MeV, 6.435 + 6.450 MeV, and 6.521 + 6.557 MeV). Each distribution is compared with $l=0$ (dotted line), $l=1$ (dashed line), and $l=2$ (solid line) DWBA calculations. The strong transition to the level at 7.413 MeV would appear to be a sum of $l=0$ and $l=1$ transitions. Such a combination requires two separate states.

The last figure of ^{23}Na(^{3}He, α)^{22}Na angular distributions (Fig. 6) shows weaker transitions whose distributions are not characteristic of simple pickup.

Relative spectroscopic strengths (NC^2S_{lj}), calculated using Eq. 1, are given in Table III. The (^{3}He, α) normalization factor, N, is not well

FIG. 7. Binding energies of proton states (right) as calculated in a deformed Woods-Saxon potential (Refs. 1 and 25). Also shown (left) for comparison are deformed harmonic-oscillator calculations (Ref. 26). The results are shown for positive deformations as a function of the Nilsson ellipsoidal deformation parameter δ.

known. Experimental estimates[22, 28, 29] range from 20 to 50, whereas theoretical estimates until recently[30, 31] have been consistently a factor of 3–10 below the experimentally obtained values. An empirical normalization was derived using the rotational-band sum rule for pickup (Table II). Values of the normalization constants determined from known bands[1, 2, 5, 6] are given in Table IV. The normalization constant for the $K = 0$, $T = 1$ band based on the 0.657-MeV level represents an upper limit, since the 1.937- and 1.952-MeV states were not resolved. These empirically determined values of N are consistent with a value of $N = 47$ determined from s-d-shell pickup in a ^{20}Ne(^{3}He, α)^{19}Ne study[22] using the same optical-model parameters. Spectroscopic factors calculated assuming $N = 52.5$ will be used (except where otherwise stated) in the following discussion and conclusions. An uncertainty of 35% is assigned to the measured spectroscopic factor when only one l contributes to the transition. When the transition proceeds by two l values, a 50% uncertainty is assigned because of errors induced in the empirical separation.

Table V presents upper limits on (^{3}He, α) spectroscopic factors for the levels whose angular distributions are shown in Fig. 5. These distributions were not characteristic of $l = 0$, 1, 2, or 0 + 2 admixed.

Information regarding removing a neutron from the ^{23}Na ground state may be obtained using the appropriate single-nucleon-pickup sum rule[32]:

$$\sum C^2 S_{lj} = N_{lj} . \qquad (4)$$

The sum extends over all states with the same l and j. N_{lj} is the number of neutrons in the lj orbi-

TABLE IV. ^{23}Na(^{3}He, α)^{22}Na empirical normalization constants, calculated using the inband sum rules of Table II.

Configuration	E_x	J^π	K^π	T	N
$(\frac{3}{2}^+ [211])^2$	0.0	3^+	3^+	0	52.5
	0.891	4^+			
$(\frac{3}{2}^+ [211])^2$	0.583	1^+	0^+	0	48.
	1.984	3^+			
$(\frac{3}{2}^+ [211])^2$	0.657	0^+	0^+	1	<73.[a]
	1.952	2^+			
	4.069	4^+			
$\frac{3}{2}^+ [211], \frac{1}{2}^- [101]$	2.211	1^-	1^-	0	43.6[b]
	2.572	2^-			
	3.521	3^-			

[a] Represents an upper limit since the 1.937- and 1.952-MeV levels were not resolved. The 1.937-MeV level is not in this rotational band.

[b] Could be low due to a mixture of other configuration in these states (see Sec. V B).

tal in the ^{23}Na ground state. The summed $l = 0$, 1, and 2 ^{23}Na(^{3}He, α) spectroscopic strengths up to an excitation of 7.51 MeV are presented in Table VI. The spectroscopic factors for the levels that are not characteristic of a particular l transfer (see Fig. 5 and Table V) are not included in the sums. Where two j's are possible, i.e., $j = l \pm \frac{1}{2}$, the summed spectroscopic strengths are tabulated based on DWBA calculations for both j's. Assuming that the ground state of ^{23}Na has four neutrons in the $2s$-$1d$ shell, the sum of $N_{l=2, j}$ and $N_{l=0, j=1/2}$ should equal four. Since the ground state of ^{23}Na contains only a small $1d_{3/2}$ component, the $2s$-$1d$ spectroscopic strength is probably not completely exhausted below 7.5 MeV. The $l = 0$ strength represents a measure of the amount of $2s_{1/2}$ neutron configuration in the ground state of ^{23}Na.

^{23}Na(^{3}He, α)^{22}Na spectroscopic factors calculated using Eq. (3) and deformed Woods-Saxon potential wave functions for protons[1] are presented in Table
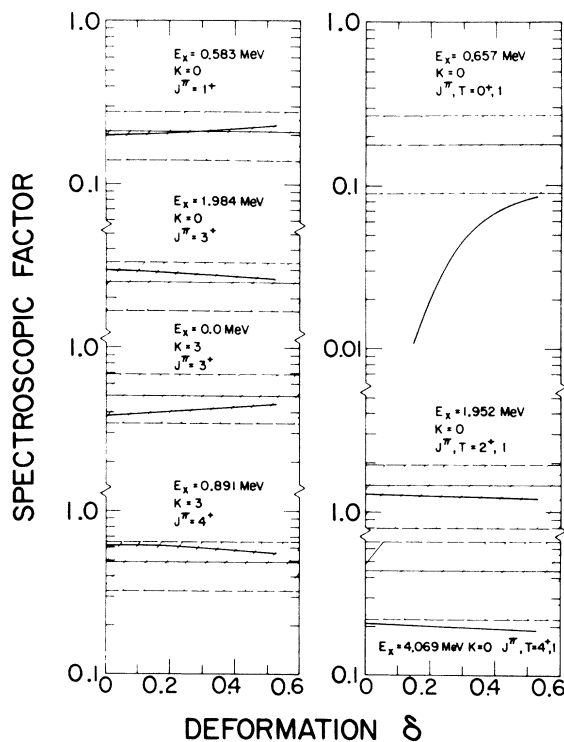

FIG. 8. Comparison of predicted and measured $l = 2$ spectroscopic factors for states based on the $(\frac{3}{2}^+ [211])^2$ Nilsson configuration. The solid horizontal lines are the experimental values (based on a normalization constant of 52.5 — see Table IV and text) and the dashed area represents the assigned errors. When it is possible for the transfer to proceed by two j's, the experimental value shown corresponds to the j having the larger predicted spectroscopic factor. The curves are predictions of the rotational model (see text) as a function of deformation. See Sec. V A of the text for discussion.

VII. The proton and neutron wave functions for otherwise identical quantum numbers are the same to within 10% in amplitude for any component.[1,2] The calculations were based on the ^{23}Na ground state having one proton and two neutrons in the $\frac{3}{2}^{+}[211]$ Nilsson orbit and all lower orbits filled (Fig. 7). Whenever a specific final state of ^{22}Na can be associated with a particular member of a rotational band, its experimental excitation energy is listed in column 4 and its measured spectroscopic factor is listed in column 5. When it was possible for the pickup to proceed by two j's, the tabulated spectroscopic factor, S_{exp}, is for the j predicted to have the larger spectroscopic factor, S_{th}. If two j's contribute, the sum of the S_{th}'s should be compared with S_{exp}. The tabulated experimental spectroscopic factors are based on a normalization constant of $N = 52.5$ (determined from the ground-state-band sum rule – Table IV).

V. DISCUSSION

A. Positive-Parity States

Three positive-parity rotational bands ($K = 0$, $T = 0$; $K = 0$, $T = 1$; and $K = 3$, $T = 0$) based on two nucleons in the $\frac{3}{2}^{+}[211]$ Nilsson orbit outside a ^{20}Ne core have previously been suggested.[1,2,5,6] Figure 8 compares predicted and measured ^{23}Na-(^{3}He, α) $l = 2$ spectroscopic factors for the levels

in these bands that may be populated by single-neutron pickup from the ground state of ^{23}Na. (The transition to the $J^{\pi} = 2^{+}$, $T = 1$ level at 1.952 MeV is not included, since the α particles corresponding to this transition are not resolved from those for the transition to the 1.937-MeV level.) The solid horizontal lines are the experimental spectroscopic factors, and the hatched area corresponds to the assigned errors. The measured spectroscopic factors are based on a normalization constant, N, of 52.5 (see Table IV). When it is possible for the transfer to proceed by two j's, the spectroscopic factors shown correspond to the j-value having the larger predicted spectroscopic factor (Table VII). The curves in Fig. 8 are the predicted spectroscopic factors as a function of the deformation. With the exception of the transition to the level at 0.657 MeV, these predicted spectroscopic factors are not strong functions of deformation, and the agreement of the predicted and measured spectroscopic factors is satisfactory for all deformations. For the transition to the 0.657-MeV level, satisfactory agreement is obtained only for large deformations, i.e., $\delta \gtrsim 0.5$. This large deformation is consistent with previous studies in this mass region.[1,2,6–9] The (^{3}He, α) transitions to states based on this configuration are predicted to proceed by pure $l = 2$ transfer, since a neutron is removed from a Nilsson orbit having $\Omega^{\pi} = \frac{3}{2}^{+}$. No $l = 0$ com-

TABLE V. Upper limit of ^{23}Na(^{3}He, α)^{22}Na spectroscopic factors for transitions to levels shown in Fig. 5.

Level No.	E_x (MeV)	l_n	j_n	NC^2S	Level No.	E_x (MeV)	l_n	j_n	NC^2S
32 + 33	5.734 ± 5.745	2	$\frac{5}{2}$	1.62	47	6.582	2	$\frac{5}{2}$	1.65
			$\frac{3}{2}$	2.32				$\frac{3}{2}$	2.56
		1	$\frac{3}{2}$	1.20			1	$\frac{3}{2}$	2.04
			$\frac{1}{2}$	1.60				$\frac{1}{2}$	2.74
		0	$\frac{1}{2}$	0.82			0	$\frac{1}{2}$	4.60
43 + 44	6.435 ± 6.450	2	$\frac{5}{2}$	1.72	56	7.081	2	$\frac{5}{2}$	1.83
			$\frac{3}{2}$	2.64				$\frac{3}{2}$	2.96
		1	$\frac{3}{2}$	1.70			1	$\frac{3}{2}$	1.72
			$\frac{1}{2}$	2.24				$\frac{1}{2}$	2.36
		0	$\frac{1}{2}$	1.14			0	$\frac{1}{2}$	0.38
45 + 46	6.521 ± 6.557	2	$\frac{5}{2}$	4.68	62	7.413	2	$\frac{5}{2}$	6.00
			$\frac{3}{2}$	7.40				$\frac{3}{2}$	9.20
		1	$\frac{3}{2}$	4.20			1	$\frac{3}{2}$	5.20
			$\frac{1}{2}$	5.20				$\frac{1}{2}$	9.00
		0	$\frac{1}{2}$	0.85			0	$\frac{1}{2}$	1.56

ponents were observed for the transitions to the states based on the $(\frac{3}{2}^{+}[211])^{2}$ configuration (Fig. 3 and Table III). The experimental spectroscopic factor for the state at 1.984 MeV is in excellent agreement with the 3^{+} member of the $K = 0$, $T = 0$ band of the $(\frac{3}{2}^{+}[211])^{2}$ Nilsson configuration. This agreement supports the 3^{+} assignment[1,2,6] for this level.

Levels at 1.937, 3.059, 3.944, and 4.360 MeV for which configurations have been suggested from the ^{21}Ne(^{3}He, d)^{22}Na study[1] were only weakly excited by the ^{23}Na(^{3}He, α)^{22}Na reaction. In all cases the suggested configurations include a particle in an orbit above the $\frac{3}{2}^{+}[211]$ Nilsson orbit (Fig. 7). Based on the assumed model of the ^{23}Na ground state and ignoring interband mixing, such states should not be excited by neutron pickup. For the same reasons, states at 5.165 and 5.995 MeV[1] should not be excited in the (^{3}He, α) reaction (the latter state has been suggested[1] as a possible doublet). The moderate spectroscopic strengths observed for these states indicate increased final-state mixing for higher excitations.

For a deformation of $\delta = 0.5$, the pure rotational model (see Fig. 7) predicts that states based on a $\frac{3}{2}^{+}[211]$, $\frac{1}{2}^{+}[220]$ configuration would be at an excitation of ~7 MeV. Since band mixing is probably severe at these excitations, no attempt has been made to associate specific states of ^{22}Na with the two bands based on this configuration. The predicted $T = 0$ (^{3}He, α) spectroscopic factors for this configuration are, however, included in Table VII. The states at 6.664, 7.008, and 7.278 MeV, populated moderately by the (^{3}He, α) reaction (Table III), probably contain some of the $\frac{1}{2}^{+}[220]$ hole strength.

B. Negative-Parity States

A negative-parity $K = 1$ band composed of states at E_{x} (in MeV), $J^{\pi} = 2.211$, 1^{-}; 2.572, 2^{-}; and 3.521, 3^{-} has previously been suggested.[1,2,5,6]

TABLE VI. Summed spectroscopic strengths.

l	Assumed j	$\sum N C^{2}S_{lj}$	$\sum C^{2}S_{lj}$ [a]
2	$\frac{5}{2}$	152.	2.90
	$\frac{3}{2}$	231.	4.40
1	$\frac{3}{2}$	62.0	1.18
	$\frac{1}{2}$	80.6	1.54
0	$\frac{1}{2}$	8.72	0.17

[a] Based on $N = 52.5$ as determined from ground-state-band sum rule (see Table IV).

These states were weakly excited by the ^{21}Ne-(^{3}He, d) reaction[1]; but they were populated strongly by the ^{23}Na(^{3}He, α) reaction (Table III). Their dominant configuration is probably a hole in the $\frac{1}{2}^{-}[101]$ Nilsson orbit. The left-hand side of Fig. 9 compares the predicted spectroscopic factors of the 1^{-}, 2^{-}, and 3^{-} states of the $K = 1$ rotational band based on the $\frac{3}{2}^{+}[211]$, $\frac{1}{2}^{-}[101]$ configuration with the experimental values for these states. The agreement is satisfactory for the 1^{-} and 2^{-} states. The angular distribution corresponding to the 3^{-} state at 3.521 MeV, however, is not characteristic of $l = 1$ pickup (Fig. 6) and the upper limit for its $l = 1$ spectroscopic factor is less than that predicted for deformation of $\delta \gtrsim 0.25$. Configuration mixing could account for the observed weak transition to this 3^{-} state [e.g. small ^{21}Ne(^{3}He, d) transitions were observed[1] to the states of this negative-parity band indicating some mixing]. Significant inter-shell mixing, however, was not predicted by the deformed Woods-Saxon potential calculation[1,2,25] which includes mixing among the lowest 13 major shells. The 3^{-} state may be populated by pickup only from a $j_{n} = \frac{3}{2}$ p-shell level, whereas 1^{-} and 2^{-} states may be populated by both $p_{1/2}$ and $p_{3/2}$ pickup. Hence the 3^{-} state is sensitive to the relative
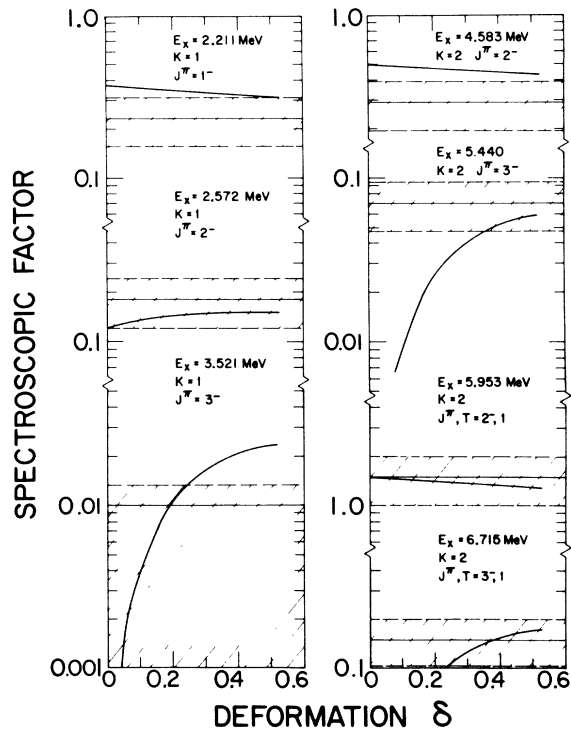

FIG. 9. Comparison of predicted and measured spectroscopic factors for states based on the $\frac{3}{2}^{+}[211]$, $\frac{1}{2}^{-}[101]$ Nilsson configuration. The description is the same as Fig. 8. See Sec. V B of the text for discussion.

TABLE VII. Comparison of measured and predicted ^{23}Na(^{3}He, α)^{22}Na spectroscopic factors.

Configuration $(\Omega^\pi[Nn_z\Lambda])$	K	J^π; T	E_x (MeV)	S_{exp}[a]	l	j	S_{th}[b] $\delta=0.0$	$\delta=0.2625$	$\delta=0.525$
$(\frac{3}{2}^+[211])^2$	3	3^+; 0	0.0	0.51	2	$\frac{5}{2}$	0.38	0.36	0.33
						$\frac{3}{2}$	0.00	0.05	0.12
		4^+; 0	0.891	0.49	2	$\frac{5}{2}$	0.62	0.60	0.55
$(\frac{3}{2}^+[211])^2$	0	0^+; 1	0.657	<0.18	2	$\frac{3}{2}$	0.00	0.04	0.09
		2^+; 1	1.952	<1.47	2	$\frac{5}{2}$	1.28	1.22	1.13
						$\frac{3}{2}$	0.00	0.04	0.08
		4^+; 1	4.069	0.44	2	$\frac{5}{2}$	0.21	0.20	0.19
$(\frac{3}{2}^+[211])^2$	0	1^+; 0	0.583	0.21	2	$\frac{5}{2}$	0.20	0.19	0.18
						$\frac{3}{2}$	0.00	0.02	0.05
		3^+; 0	1.984	0.25	2	$\frac{5}{2}$	0.30	0.28	0.26
						$\frac{3}{2}$	0.00	<0.01	<0.01
$(\frac{3}{2}^+[211], \frac{1}{2}^+[220])$	1	1^+; 0			2	$\frac{5}{2}$	0.02	0.02	0.01
						$\frac{3}{2}$	0.00	0.01	0.02
					0	$\frac{1}{2}$	0.00	0.07	0.10
		2^+; 0			2	$\frac{5}{2}$	0.16	0.12	0.09
						$\frac{3}{2}$	0.00	0.01	0.04
					0	$\frac{1}{2}$	0.00	0.02	0.03
		3^+; 0			2	$\frac{5}{2}$	0.22	0.17	0.12
						$\frac{3}{2}$	0.00	0.00	0.01
		4^+; 0			2	$\frac{5}{2}$	0.09	0.07	0.05
$(\frac{3}{2}^+[211], \frac{1}{2}^+[220])$	2	2^+; 0			2	$\frac{5}{2}$	0.07	0.05	0.04
						$\frac{3}{2}$	0.00	0.01	0.04
					0	$\frac{1}{2}$	0.00	0.10	0.14
		3^+; 0			2	$\frac{5}{2}$	0.25	0.19	0.14
						$\frac{3}{2}$	0.00	0.01	0.04
		4^+; 0			2	$\frac{5}{2}$	0.18	0.13	0.10
$(\frac{3}{2}^+[211], \frac{1}{2}^-[101])$	1	1^-; 0	2.211	0.23	1	$\frac{3}{2}$	0.00	0.02	0.04
						$\frac{1}{2}$	0.37	0.32	0.28
		2^-; 0	2.572	0.18	1	$\frac{3}{2}$	0.00	0.04	0.06
						$\frac{1}{2}$	0.12	0.11	0.09
		3^-; 0	3.521	<0.01	1	$\frac{3}{2}$	0.00	0.01	0.02
$(\frac{3}{2}^+[211], \frac{1}{2}^-[101])$	2	2^-; 0	4.583	0.29	1	$\frac{3}{2}$	0.00	0.04	0.06
						$\frac{1}{2}$	0.50	0.43	0.37
		3^-; 0	5.440	0.07	1	$\frac{3}{2}$	0.00	0.03	0.06
$(\frac{3}{2}^+[211], \frac{1}{2}^-[101])$	1	1^-; 1			1	$\frac{3}{2}$	0.00	0.06	0.11
						$\frac{1}{2}$	1.12	0.96	0.84

TABLE VII *(Continued)*

Configuration $(\Omega^{\pi}[Nn_z\,\Lambda])$	K	J^{π}; T	E_x (MeV)	S_{exp} [a]	l	j	S_{th} [b] $\delta = 0.0$	$\delta = 0.2625$	$\delta = 0.525$
		2^-; 1			1	$\frac{3}{2}$	0.00	0.11	0.18
						$\frac{1}{2}$	0.38	0.32	0.28
		3^-; 1			1	$\frac{3}{2}$	0.00	0.04	0.07
$(\frac{3}{2}^+[211], \frac{1}{2}^-[101])$	2	2^-; 1	5.953	1.51	1	$\frac{3}{2}$	0.00	0.11	0.18
						$\frac{1}{2}$	1.50	1.28	1.12
		3^-; 1	6.715	0.15	1	$\frac{3}{2}$	0.00	0.11	0.18

[a] Spectroscopic factors from Table III for $N = 52.5$. When it is possible for a transfer to proceed by two j values for the same l ($j = l \pm \frac{1}{2}$), the tabulated S_{exp} corresponds to the j that is predicted to have the larger S. S_{exp} should then be compared with the sum of the two S_{th}'s for that l.

[b] Calculated using Eq. (3) and finite-well Nilsson wave functions for given deformations. (See text and Ref. 1.)

admixture of $p_{1/2}$ and $p_{3/2}$ in the $\frac{1}{2}^-[101]$ Nilsson orbit. The 1^- and 2^- states are relatively insensitive to such a mixture, since the $\frac{1}{2}^-[101]$ Nilsson orbit is predominantly $1p_{1/2}$ for all deformations.[1] Thus a change in the $p_{3/2}$ strength in the $\frac{1}{2}^-[101]$ Nilsson orbit would change the predicted spectroscopic factor for the 3^- state at 3.521 MeV by a large amount while only affecting the predicted values for the 1^- and 2^- states slightly. Use of the normalization constant derived from the in-band sum rule (Table II) for the negative-parity band (Table IV) would increase the experimental spectroscopic factors (by about 20%) giving better agreement for the 1^- and 3^- states, but poorer agreement for the 2^- state.

The two ^{22}Na levels at $E_x = 4.583$ and 5.440 MeV, having angular distributions characteristic of $l = 1$ neutron pickup, are suggested for the 2^- and 3^- levels of a $K = 2$ band based on the same $\frac{3}{2}^+[211]$, $\frac{1}{2}^-[101]$ configuration. The agreement between the predicted and measured spectroscopic strengths (Fig. 9) would be even better if the normalization constant derived from the known $K^{\pi} = 1^-$ band were used (Table IV). The levels at 5.953 and 6.715 MeV are suggested (Fig. 9) as the $T = 1$ components of the $K = 2$ band of this same configuration. Neither of these levels is significantly populated by the ^{20}Ne(^{6}Li, α) reaction[2] which should populate only $T = 0$ states in ^{22}Na. Further evidence supporting the identification of the 5.953-MeV state as the analog of the 5.14-MeV, 2^- level in ^{22}Ne[33] is presented in Sec. V C. The 6.715-MeV state in ^{22}Na is at the proper excitation to be the analog of the 6.12-MeV, (3^-) level[33] in ^{22}Ne.

The level at 6.326 MeV, which was populated by a strong $l = 1$ transition in the ^{21}Ne(^{3}He, d) reaction,[1] is only moderately excited in the present study (see Fig. 4 and Table III). This is consistent with the suggestion[1] that the predominant configu-

ration of this state is unpaired nucleons in the $\frac{3}{2}^+[211]$ and $\frac{1}{2}^-[330]$ Nilsson orbits outside a ^{20}Ne core.

C. Comparison with Other Data

Table VIII compares the spectroscopic factors of the ^{23}Na(d, ^{3}He)^{22}Ne reaction at 34.5-MeV incident energy[34] with the $T = 1$ spectroscopic factors of this study. The agreement is within the normal DWBA uncertainties except for the one negative-parity state at 5.953 MeV in ^{22}Na. The (^{3}He, α) spectroscopic factor for this level is in good agreement with the predicted value for a deformation of $\delta \approx 0.5$, whereas the (d, ^{3}He) value is too high by almost a factor of 2.

Table IX compares the spectroscopic factor of this study with those of the ^{23}Na(p, d)^{22}Na[18] and ^{23}Na(d, t)^{22}Na[19,20] reactions. The (p, d) data is in excellent agreement with the present study for the positive-parity levels, but the negative-parity (p, d) spectroscopic factors are consistently larger than the corresponding (^{3}He, α) spectroscopic factors. The (d, t) data of Wei[20] disagrees with the present study by observing sizable $l = 0$ components in the transitions to the levels at $E_x = 0.583$ and 1.984 MeV. The $l = 0$ (d, t) component for the 1.984-MeV transition is also inconsistent with the $L = 4$ angular distribution observed for this level in the ^{20}Ne(^{3}He, p)^{22}Na study[2] and with the γ decay[6] of the 1.984-MeV level.

VI. CONCLUSIONS

The measured spectroscopic factors for the three lowest rotational bands and the calculated spectroscopic factors for states based on the $(\frac{3}{2}^+[211])^2$ configuration agree (within the uncertainties of the DWBA calculations) for deformations of order $\delta \approx 0.5$ (see Fig. 8). This value for the deformation is in agreement with previous measure-

TABLE VIII. Comparison of ^{23}Na(^{3}He, α)^{22}Na and ^{23}Na(d, ^{3}He)^{22}Ne spectroscopic factors.

^{23}Na(^{3}He, α)^{22}Na [a]			^{23}Na(d, ^{3}He)^{22}Ne [b]			Theory [c]
E_x (MeV)	$S(0)$	$S(2)$	E_x (MeV)	$S(0)$	$S(2)$	$S(2)$
0.657	$\cdots$	<0.18	g.s.	$\cdots$	0.12	0.09
1.952	$\cdots$	<1.47	1.28	<0.3	1.65–1.77	1.21
4.069	$\cdots$	0.44	3.35	$\cdots$	0.60±0.12	0.19
5.165	0.18	0.40	4.47	0.12–0.20	0.22–0.45	$\cdots$
5.953	$S(1)=1.51$		5.14	$S(1)=2.55$		$S(1)=1.30$

[a] Present work, $N = 52.5$.
[b] Reference 34.
[c] Based on Eq. (3) and finite-well Nilsson wave function for a deformation of $\delta = 0.525$.

ments for this mass region.[1,2,6-9] The observed spectroscopic factors for the three negative-parity rotational bands (except for the 3⁻ state at 3.521 MeV) are in agreement with the predicted values for a similar value of the deformation, i.e., δ ≈ 0.5. The transition to the 3.521-MeV level was weak, and its angular distribution is not characteristic of direct neutron pickup (see Fig. 6). The upper limit placed on the $l = 1$ spectroscopic factor for this 3⁻ state is less than the predicted values for deformations of $\delta \gtrsim 0.25$. Possible explanations for such a discrepancy are discussed above in Sec. VB. The observed spectroscopic factor for another suggested 3⁻ state observed at $E_x = 5.440$ MeV is in agreement with the value predicted by the rotational model for the 3⁻ state in the $K^\pi = 2^-$, $T = 0$ band based on the $\frac{3}{2}^+[211]$, $\frac{1}{2}^-[101]$ configuration. The total strength for the 2⁻ and 3⁻ states suggested as being based on the $T = 0$ part of this configuration is in excellent agreement with the predictions of the rotational model for large deformations (see Fig. 9).

The suggested negative-parity rotational bands in ^{22}Na are summarized in Fig. 10. The Nilsson configuration and K and T quantum numbers for each band are given below the band head. The $K^\pi = 1^-$, $T = 0$ band based on the $\frac{3}{2}^+[211]$, $\frac{1}{2}^-[101]$ configuration has been previously suggested.[1,4-6] The $K^\pi = 2^-$, $T = 0$ and 1 bands are discussed in Sec. V. A $K^\pi = 1^-$, $T = 1$ band based on this same $\frac{3}{2}^+[211]$, $\frac{1}{2}^-[101]$ configuration would be predicted to lie above the $K = 2$, $T = 1$ band. The splitting of the $T = 0$, $K^\pi = 1^-$ and 2⁻ band heads of this configuration (~2.4 MeV) suggests that the band head of the $K = 1$, $T = 1$ band in ^{22}Na might be above 8 MeV in excitation. The $K = 1$, $T = 1$ rotational band based on this configuration is not presently known in ^{22}Ne, but several negative-parity states are known[35] in ^{22}Ne above 7 MeV. The association of the 6.326-MeV level with one of the band heads of the $\frac{3}{2}^+[211]$, $\frac{1}{2}^-[330]$ particle configuration was suggested by Ref. 1.

The positive-parity rotational bands have previously been summarized in Ref. 1. The results of the present work are consistent with the positive-parity identification suggested therein.

The results of the present study and of the ^{21}Ne-(^{3}He, d) single-particle-stripping reaction[1] are compared in Table X along with a summary of the spins, parities, and suggested configurations of the states of ^{22}Na. The spectroscopic factors tabulated are for $j = \frac{5}{2}$ ($l = 2$) and $j = \frac{1}{2}$ ($l = 1$) except where the other j transferred is known to be stronger (see Ref. 1 and Table III). Where the reaction is known to proceed by both $l = 0$ and 2, the spectroscopic factor corresponding to the $l = 0$ component is presented first. Tabulated spectroscopic factors were calculated using normalization constants, $N = 52.5$ for (^{3}He, α) (see Table IV)

TABLE IX. Comparison of spectroscopic factors for single-neutron pickup from ^{23}Na.

E_x (MeV)	l_n	j_n	C^2S (^{3}He, α) [a]	(p,d) [b]	(d,t) [c]	(d,t) [d]
g.s.	2	$\frac{5}{2}$	0.52	0.52		0.52
0.583	2	$\frac{5}{2}$	0.21	0.20		
	0	$\frac{1}{2}$	<0.02	<0.10	0.14	0.17 $l=2$
0.657	2	$\frac{3}{2}$	≤0.06	≤0.07		
0.891	2	$\frac{5}{2}$	0.49	0.56		0.30
1.937 / 1.952	2	$\frac{5}{2}$	0.49	0.70±0.20 $l=2$		
1.984	2	$\frac{5}{2}$	0.25	≤0.08 $l=0$		
	0	$\frac{1}{2}$	<0.02		0.08	
2.211	1	$\frac{1}{2}$	0.23	0.31		
2.572	1	$\frac{1}{2}$	0.18	0.28		

[a] Present study, $N = 52.5$.
[b] Reference (18) normalized to S(g.s.) = 0.52.
[c] Reference (20).
[d] Reference (19) normalized to S(g.s.) = 0.52.

TABLE X. Summary of single-particle transitions leading to the final states of ²²Na.

Level No.	E_x [a] (MeV)	J^π; T [b]	^{21}Ne(^{3}He, d) l_p	$(2J_f+1)C^2S$ [c]	^{23}Na(^{3}He, α) l_n	C^2S [d]	K	Configuration Ω^π $[Nn_z\Lambda]$
0	0.0	3^+	2	1.66	2	0.51	3	$(\frac{3}{2}^+ [211])^2$
1	0.583	1^+	(0)+2	(0.058)+0.977	2	0.21	0	$(\frac{3}{2}^+ [211])^2$
2	0.657	0^+; 1	2	<0.203	2	<0.06	0	$(\frac{3}{2}^+ [211])^2$
3	0.891	4^+	2	3.75	2	0.49	3	$(\frac{3}{2}^+ [211])^2$
4	1.528	5^+	e		e		3	$(\frac{3}{2}^+ [211])^2$
5	1.937	1^+	0+2	0.293+2.50	2	0.49	1	$\frac{3}{2}^+ [211]$, $\frac{1}{2}^+ [211]$
6	1.952	2^+; 1					0	$(\frac{3}{2}^+ [211])^2$
7	1.984	3^+	2	0.934	2	0.25	0	$(\frac{3}{2}^+ [211])^2$
8	2.211	1^-	1	0.045	1	0.23	1	$\frac{3}{2}^+ [211]$, $\frac{1}{2}^- [101]$
9	2.572	2^-	1	0.047	1	0.18	1	$\frac{3}{2}^+ [211]$, $\frac{1}{2}^- [101]$
10	2.969	3^+	2	0.793	(2)	<0.02	f	f
11	3.059	2^+	0+2	0.306+0.956	2	0.03	(1)	$(\frac{3}{2}^+ [211]$, $\frac{1}{2}^+ [211])$
12	3.521	3^-	(1)	<0.009	g	<0.01	1	$\frac{3}{2}^+ [211]$, $\frac{1}{2}^- [101]$
13	3.708	(6^+)	e		e		(3)	$((\frac{3}{2}^+ [211])^2)$
14	3.944	1^+	0+2	0.152+0.495	0	0.03	(1)	$(\frac{3}{2}^+ [211]$, $\frac{5}{2}^+ [202])$
15	4.069	$(4)^+$; (1)	2	0.185	2	0.15	(0)	$((\frac{3}{2}^+ [211])^2)$
16	4.294		h		h			
17	4.319	1^+	(2)	0.038	e			
18	4.360	$2^+(1^+)$	0	1.66	0+2	0.02+0.02	(2(1))	$(\frac{3}{2}^+ [211]$, $\frac{1}{2}^+ [200])$
19	4.466		e		e			
20	4.522		e		e			
21	4.583	$2^-(0^-, 1^-, 3^-)$	(0) [i]	0.06	1	0.29	2	$\frac{3}{2}^+ [211]$, $\frac{1}{2}^- [101]$
22	4.622	1	j		e			
23	4.708	$(3^+, 4^+, 5^+)$	h		e			
24	4.770	$0^+, 1^+, 2^+, 3^+, 4^+$	2	0.467	(2)	0.08	f	f
25	5.061	$1^+, 2^+$	k		0+2	0.01+0.02		
26	5.099		k					
27	5.117				g			
28	5.165	$(2)^+$; (1)	0+2	0.319+0.494	0+2	0.06+0.13	2	$\frac{3}{2}^+ [211]$, $\frac{1}{2}^+ [211]$
29	5.317	$1^+, 2^+(0^+, 3^+, 4^+)$	(0)+2	(0.065)+0.260	e			
30	5.440	$3^-(0^-, 1^-, 2^-)$	1	0.152	1	0.07	2	$\frac{3}{2}^+ [211]$, $\frac{1}{2}^- [101]$
31	5.605	$1^+, 2^+$	0+2	0.044+0.104	0+2	0.01+0.02		
32	5.734	One state $0^+, 1^+$	k		k			
33	5.745							
34	5.830	$1^+, 2^+$	k		e			
35	5.858				0+2	<0.01+0.02		
36	5.938		m		m			
37	5.953	$2^-(0^-, 1^-, 3^-)$; (1)	m		1	0.50	2	$\frac{3}{2}^+ [211]$, $\frac{1}{2}^- [101]$
38	5.995 [n]	$1^+, 2^+$	0+2	1.41+1.99	2	0.11	1(2)	$(\frac{3}{2}^+ [211]$, $\frac{1}{2}^+ [200])$

TABLE X *(Continued)*

Level No.	E_x [a] (MeV)	J^π; T [b]	^{21}Ne(^{3}He, d) l_p	$(2J_f+1)C^2S$ [c]	^{23}Na(^{3}He, α) l_n	C^2S [d]	K	Configuration $\Omega^\pi[Nn_z\Lambda]$
39	6.088 [n]	1^+, 2^+	(0)+2	(0.362)+0.695	0+2	<0.01+0.02		
40	6.185 [n]	0^+, 1^+, 2^+, 3^+, 4^+	2	3.09	(2)	0.04		
41	6.247		j		e			
42	6.326	1^-, $2^-(0^-$, $3^-)$	1	0.561	(1)	0.16	1, 2	$\frac{3}{2}^+$ [211], $\frac{1}{2}^-$[330]
43	6.435 ⎫		k		k			
44	6.450 ⎭							
45	6.521		m	⎫	k			
46	6.557	1^+, 2^+	0+2	0.455+0.528 ⎭				
47	6.582				k			
48	6.640				e			
49	6.664	1^+, $2^+(3^+)$			(0+2)	0.03+0.04		
50	6.715	$3^-(0^-$, 1^-, $2^-)$; (1)			(1)	0.05	2	$\frac{3}{2}^+$ [211], $\frac{1}{2}^-$[101]
51	6.750				e			
52	6.834	$0^+(1^+)$; (1)			h			
53	6.862				e			
54	6.961				e			
55	7.008	0^+, 1^+, 2^+, 3^+, 4^+			2	0.09		
56	7.081				k			
57	7.153				e			
58	7.220				e			
59	7.242				h			
60	7.278	0^+, 1^+, 2^+, 3^+, 4^+			2	0.13		
61	7.367				e			
62	7.413				k			
63	7.512	1^+, 2^+			0	<0.01		

[a] Energies are taken from sources listed in Table III.

[b] Assignments as summarized in Table III.

[c] From Ref. 1 spectroscopic strengths for $j=\frac{5}{2}$ ($l=2$) and $j=\frac{1}{2}$ ($l=1$) except where other j is known to be predominant.

[d] From Table III with $N=52.5$ (see Table IV). Spectroscopic strengths for $j=\frac{5}{2}$ ($l=2$) and $j=\frac{1}{2}$ ($l=1$) except where other j is known to be predominant.

[e] No direct-transfer pattern observed.

[f] Both 2.969- and 4.770-MeV levels are considered to be equally likely candidates for the 3^+ member of the $K=1$, $T=0$ band based on the $\frac{3}{2}^+$ [211], $\frac{1}{2}$ [211] configuration (see Ref. 1).

[g] No direct-transfer pattern observed; however, an upper limit for $l=1$ transfer is given because of the known $J^\pi = 3^-$.

[h] State not excited.

[i] See text.

[j] State covered by impurity.

[k] Direct-transfer-like pattern observed, but not characteristic of $l=0$, 1, 2, or 0+2.

[m] Covered by neighboring strongly excited state.

[n] Possible doublet.

6.71   3⁻(0,1,2)

6.33   1,2⁻(0,3⁻)
K=1 or 2   T=0
1/2⁻ [330]

5.95   2⁻(0,1,3⁻)
K=2   T=1
1/2⁻ [101]

5.44   3⁻(0,1,2⁻)

4.58   2⁻(0,1,3)
K=2   T=0
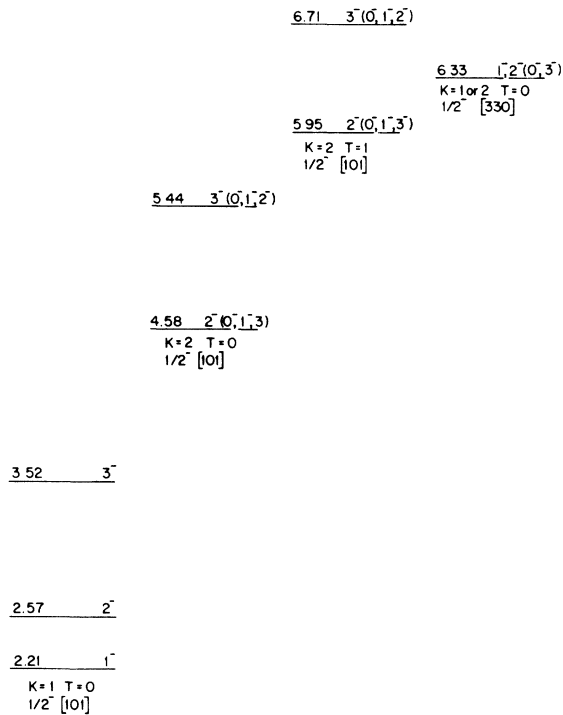1/2⁻ [101]

3.52   3⁻

2.57   2⁻

2.21   1⁻
K=1   T=0
1/2⁻ [101]

FIG. 10. Summary of suggested negative-parity rotational bands in ^{22}Na. The assumed configuration of each band is an unpaired nucleon in the $\frac{3}{2}^+$ [211] Nilsson orbit coupled to an unpaired nucleon in the orbit listed for each band.

and $N = 4.42$ for (^{3}He, d).[1] A discrepancy exists between the (^{3}He, d) and (^{3}He, α) results for the level at an excitation of 4.583 MeV. Since the $l = 0$ (^{3}He, d) transition was very weak,[1] the assignment in Table X is based on the stronger $l = 1$ (^{3}He, α) transition (see Fig. 4). A possible explanation of this discrepancy would be a closely spaced doublet. The observed $l = 1$ ^{21}Ne(^{3}He, d)[1] and ^{23}Na-(^{3}He, α) transitions to the level at 2.572 MeV are consistent with the 2⁻ assignment[5] for this state and are not consistent with a recent γ-ray polarization work[36] which suggested a 2⁺ assignment for this level. That work[36] also suggested a 2⁺ assignment for the state at 1.984 MeV which is presently believed to have $J^\pi = 3^+$. The preference of $J^\pi = 3^+$ for this latter state has previously been discussed.[1, 2, 6]

In summary, configurations have been discussed for all levels of ^{22}Na observed below 4.2 MeV in excitation and for all negative-parity states obser-

ved below 7.5 MeV. Below 5.7 MeV there is some knowledge of the spins and parities of all levels except for those at 4.294, 4.466, 4.522, 5.099, and 5.117 MeV. These levels were only weakly populated in single-nucleon stripping,[1] two-nucleon stripping,[2] and in the present single-nucleon pickup. Positive-parity states having $J > 4$ and negative-parity states with $J > 3$ would not be expected to be populated by single-nucleon, s-d-shell, and p-shell transfer on $J^\pi = \frac{3}{2}^+$ targets. Thus some of the levels not populated by the ^{21}Ne(^{3}He, d)[1] and ^{23}Na(^{3}He, α) reactions probably correspond to states with higher spins. The 7⁺ member of the ground-state band and the 4⁻ member of the $K^\pi = 1^-$ band (based on the 2.211-MeV band head), for example, are predicted[5] to lie between the excitations of 4.3 and 5.3 MeV. More complicated configurations, e.g. those having two holes in the ^{20}Ne core, also would not be expected to be excited by either the single-nucleon transfer reactions or by the two-nucleon stripping reaction.

The experimental (^{3}He, α) spectroscopic factors for the states previously suggested[1] to correspond to the rotational bands based on the ($\frac{3}{2}^+$[211])^2 Nilsson configuration are in agreement with the predicted rotational-model spectroscopic factors. Only weak (^{3}He, α) transitions were observed populating levels that were suggested[1] as corresponding to an unpaired particle in a Nilsson orbit above the $\frac{3}{2}^+$[211] level. All the negative-parity levels observed in the ^{21}Ne(^{3}He, d)^{22}Na and the ^{23}Na-(^{3}He, α)^{22}Na reactions can be understood in terms of the rotational model. The deformation suggested by a comparison of predicted and observed (^{3}He, α) spectroscopic factors ($\delta \approx 0.5$) is in agreement with the ^{21}Ne(^{3}He, d) results[1] and with other recent values.[2, 6-9]

The simple rotational model is more successful in its explanation of the low-lying negative-parity single-particle states than for the positive-parity states.[1] The low-lying negative-parity states can be based on unpaired nucleons in only two Nilsson orbits, the $\frac{1}{2}^-$[101] and the $\frac{1}{2}^-$[330], which are derived from different major shells. On the other hand, positive-parity, single-particle levels can correspond to several Nilsson orbits, e.g. the $\frac{3}{2}^+$[211], $\frac{1}{2}^+$[211], $\frac{5}{2}^+$[202], $\frac{1}{2}^+$[200], or $\frac{1}{2}^+$[220], all arising from the same $N = 2$ shell. Considerable mixing would thus be expected (and indeed is observed[1]) to take place among the positive-parity levels.

*Work supported by the National Science Foundation.

†Present address: Los Alamos Scientific Laboratory, University of California, Los Alamos, New Mexico 87544.

[1] J. D. Garrett, R. Middleton, and H. T. Fortune, Phys. Rev. C **4**, 165 (1971).

[2] J. D. Garrett, R. Middleton, D. J. Pullen, S. A. Andersen, O. Nathans, and O. Hansen, Nucl. Phys. **A164**, 449 (1971).

[3] J. D. Garrett, H. T. Fortune, and R. Middleton, Bull. Am. Phys. Soc. **16**, 36 (1971).

[4] H. T. Fortune, J. D. Garrett, and R. Middleton, Bull. Am. Phys. Soc. **16**, 36 (1971).

[5] J. W. Olness, W. R. Harris, P. Paul, and E. K. Warburton, Phys. Rev. C **1**, 958 (1970).

[6] E. K. Warburton, A. R. Poletti, and J. W. Olness, Phys. Rev. **168**, 1232 (1968).

[7] B. Hausser, B. Hooton, D. Pelte, T. Alexander, and H. Evans, Phys. Rev. Letters **22**, 359 (1969).

[8] D. Schwalm and P. Povh, Phys. Letters **29B**, 103 (1969).

[9] K. Nakai, F. Stephens and R. Diamond, in *Proceedings of the International Conference on Properties of Nuclear States,* edited by A. M. Harvey *et al.* (Les Presses de l'Université de Montréal, Montréal, Canada, 1969), p. 685.

[10] E. K. Warburton, J. W. Olness, and A. R. Poletti, Phys. Rev. **160**, 938 (1967).

[11] A. R. Poletti, E. K. Warburton, J. W. Olness, and S. Hechtl, Phys. Rev. **162**, 1040 (1967).

[12] R. W. Kavanaugh, Bull. Am. Phys. Soc. **12**, 913 (1967).

[13] P. Paul, J. W. Olness, and E. K. Warburton, Phys. Rev. **173**, 1063 (1968).

[14] J. G. Pronko, C. Rolfs, and H. J. Maier, Phys. Rev. **167**, 1066 (1968).

[15] A. E. Blaugrund, A. Fischer, and A. Z. Schwarzschild, Nucl. Phys. **A107**, 411 (1968).

[16] E. K. Warburton, L. E. Carlson, G. T. Garvey, D. A. Hutcheon, and K. P. Jacksen, Nucl. Phys. **A136**, 160 (1969).

[17] K. W. Jones, A. Z. Schwarzschild, E. K. Warburton, and D. B. Fossan, Phys. Rev. **178**, 1773 (1969).

[18] R. C. Haight, Ph.D. thesis, Princeton University, 1969 (unpublished).

[19] W. T. Vogelsang and J. N. McGruer, Phys. Rev. **109**, 1663 (1958).

[20] T. Wei, Bull. Am. Phys. Soc. **12**, 85 (1968); and as quoted in Haight, Ref. 18.

[21] P. D. Kunz, University of Colorado Report No. COO-535-613 (unpublished).

[22] J. D. Garrett, R. Middleton, and H. T. Fortune, Phys. Rev. C **2**, 1243 (1970).

[23] H. Kattenborn, C. Mayer-Boricke, and B. Mertens, Nucl. Phys. **A138**, 657 (1969).

[24] G. R. Satchler, Ann. Phys. (N.Y.) **3**, 275 (1958).

[25] S. Wahlborn and G. Ehrling, to be published.

[26] B. Chi, Nucl. Phys. **83**, 97 (1966).

[27] S. Hinds, H. Marchant, and R. Middleton, Nucl. Phys. **51**, 427 (1964).

[28] T. J. Gray, H. T. Fortune, W. Trost, and N. R. Fletcher, Nucl. Phys. **A144**, 129 (1970).

[29] R. Stock, R. Bock, P. David, H. H. Duhm, and T. Tamura, Nucl. Phys. **A104**, 136 (1967).

[30] T. K. Lim, Nucl. Phys. **A129**, 259 (1969); to be published.

[31] W. J. Thompson and W. R. Hering, Phys. Rev. Letters **24**, 272 (1970).

[32] J. P. Schiffer, in *Isospin in Nuclear Physics,* edited by D. H. Wilkinson (North-Holland, Amsterdam, 1969), p. 665.

[33] R. Ollerhead, G. Allen, A. Baxter, B. Gillespie, and J. Kuehner, Bull. Am. Phys. Soc. **14**, 1221 (1969); to be published.

[34] B. H. Wildenthal and E. Newman, Phys. Rev. **175**, 1431 (1968).

[35] P. Neogy, Ph.D. thesis, University of Pennsylvania, 1970 (unpublished); P. Neogy, W. Scholz, and R. Middleton, to be published.

[36] A. M. Baxter, B. W. J. Gillespie, and J. A. Kuehner, Can. J. Phys. **48**, 2434 (1970).